Validation of Antibacterial Systems for Sustainable Ceramic Tiles

Valeria La Torre [1] (ID)**, Elisa Rambaldi** [1] (ID)**, Giulia Masi** [2]**, Silvia Nici** [3]**, Daniele Ghezzi** [4] (ID)**, Martina Cappelletti** [3] (ID)
and Maria Chiara Bignozzi [2],* (ID)

1   Centro Ceramico, Via Martelli 26, 40138 Bologna, Italy; vale.mati91@gmail.com (V.L.T.);
     rambaldi@centroceramico.it (E.R.)
2   Department of Civil, Chemical, Environmental and Materials Engineering, University of Bologna,
     Via Terracini 28, 40131 Bologna, Italy; giulia.masi5@unibo.it
3   Department of Pharmacy and Biotechnology, University of Bologna, Via Irnerio 42, 40126 Bologna, Italy;
     silvia.nici@studio.unibo.it (S.N.); martina.cappelletti2@unibo.it (M.C.)
4   Laboratory of NanoBiotechnology, IRCCS Istituto Ortopedico Rizzoli, Via di Barbiano 1/10,
     40136 Bologna, Italy; daniele.ghezzi@ior.it
*   Correspondence: maria.bignozzi@unibo.it; Tel.: +39-(05)-12090342

Abstract: Ceramic tiles are bacteriostatic materials; however, the COVID-19 emergency has pushed tile producers to improve surfaces' antibacterial properties. The aim of this work was to validate a silver-based antibacterial treatment applied to porcelain stoneware tiles based on natural and waste materials, thus correlating surface functionalization to tile composition and relevant physical, microstructural, and textural parameters. The treatment was applied before firing, with and without a polymeric primer. Antibacterial activity tests, stain resistance tests, and contact angle measurements were carried out on fired tiles. Further investigations were made by SEM and optical profilometry in order to study the morphological–structural profile of tile surfaces. Results showed strong antibacterial activities for all the functionalized tiles, which were mainly correlated to the morphological and textural parameters of ceramic surfaces, as well as the presence of the polymeric primer.

Keywords: ceramic tile; antibacterial; recycling; porcelain stoneware; silver compound; functionalization; surface treatment

1. Introduction

The current health emergency, caused by the spread of COVID-19, has drawn the attention of the scientific community to the importance of environmental health in relation to the risk of contamination of covering surfaces.

Ceramic tiles are bacteriostatic materials due to their inorganic nature and vitrified surface, which prevent the proliferation of microorganisms and pathogens, and as a result, they are easy to be hygienically cleaned by means of traditional procedures [1,2]. Since ceramic surfaces are susceptible to bacterial contamination in any destination of use, the constant removal of microbial cells from the surface is essential for the sanitization of the environment. In this perspective, the ceramic tile industry aims to process ceramic tiles to imbue the surfaces of tiles with antibacterial properties, already offering a rather wide range of treatments [3–7].

Currently, there are two main types of technologies able to actively control and remove the microbial load affecting surfaces: photocatalytic and non-photocatalytic technologies. They consist of nanostructured coatings based on titanium dioxide (TiO_2) or silver ions (Ag^+) as active agents, respectively. Both of these semiconductor materials are well known to exert a cytotoxic effect toward different species of microorganisms, causing the inhibition of pathogen proliferation [8–10].

In particular, the bactericidal effect seems to be associated with the induction of intracellular biomolecule (DNA, proteins, and lipids) damage, reactive oxygen species (ROS) generation, and cell wall disruption [10]. Several studies demonstrated that, among

the physical states under which metal oxides can interact with microbial cells, metal nanoparticles exhibit high level of antibacterial activity, due to their small size and high surface–volume ratio [11–14].

In general, TiO_2-based photocatalytic technology is limited by lighting conditions (requiring UV illumination); however, in the specific case of ceramic tiles, particular attention should be addressed to the production process. Of all the TiO_2 polymorphs, anatase is known to exert the best photocatalytic performance, secondarily followed by rutile [15,16]. The sintering thermal cycle of the ceramic body includes a temperature range (600–1100 °C) which, critically, involves the transformation of anatase into rutile, with the risk of reducing the photocatalytic efficacy. For this reason, the industrial exploitation of this technology in ceramic tiles is limited to the implementation of TiO_2-based surface treatments [16–19].

Among the non-photocatalytic technologies, silver-based soluble compounds can be applied, thus exploiting the advantageous environmental flexibility of silver, which does not require specific activation conditions. The antibacterial activity is triggered by direct physical contact with pathogens and carried out through the release of bioactive Ag^+ ions. This prerogative ensures the adaptability of silver-based technology to different application techniques, such as the production of ceramic tiles, coatings, surface treatments, or compounds added into the ceramic-body-glaze system [20–22].

Silver-based-soluble-compound antibacterial technology is already known to be effective if applied on materials other than tiles [23,24]. In this regard, several studies show that antibacterial efficacy can be achieved by designing hybrid technologies that utilize both silver and titania [25–28]. In this case, the photocatalytic aspect is based on a surface coating of ceramic materials with photoactive compounds, which, under light irradiation, produce highly ROS. In turn, pollutants or pathogenic species on the surface undergo continuous degradation processes via ROS. Thanks to the presence of Ag and TiO_2, the surface also exhibits antibacterial properties in the dark through the combined action of the photocatalytic coating and Ag.

In this study, a silver-based antibacterial formulation was applied to two types of unglazed porcelain stoneware tiles, prepared with different mixtures.

Porcelain tiles, representing almost 88% of the Italian ceramic tiles product portfolio [29], are generally characterized by a very compact structure, with extremely low porosity, thus ensuring high resistance to abrasion (surface hardness) and mechanical stress (bending and impact), as well as low frost susceptibility. Such features qualify porcelain tiles as suitable for any type of constructive solution [30,31].

Two porcelain stoneware mixtures were intentionally designed: a mix made entirely of natural raw materials (30–40 wt% ball clays, 0–10 wt% kaolin, 40–55 wt% feldspar and 0–15 wt% quartz sand) [32], and a mix based on a high content of recycled material, derived almost exclusively from the waste of the ceramic process itself. A 20 wt% of recycled ceramic material from the total recovery of unfired and fired scraps, including grinding and lapping fine powders, was used [33–35]. The mixture based on recycled raw materials was specifically developed in order to avoid modifying the settings of a real industrial ceramic production cycle.

The novelty of this work is the evaluation of the effectiveness of the investigated silver-based antibacterial treatment—applied before sintering—on the surfaces of traditional and sustainable porcelain stoneware tiles. The silver-based functionalizing treatment was applied using a screen-printing technique, with and without the addition of a polymeric primer to promote the adhesion between the ceramic substrate and the silver coating.

The effect of regular cleaning procedures (cleanability) on the silver-based treatment was assessed through a comprehensive surface analysis investigation (compositional, textural, and/or microstructural characteristics).

2. Materials and Methods

Industrial spry-dried powders of natural and recycled raw materials were used to prepare traditional and high-recycled-content mixtures, named G and R, respectively. Their chemical composition, determined by inductively-coupled plasma emission spectroscopy (ICP-OES Perkin Elmer Optima 3200XL, Waltham, MA, USA), is reported in Tables 1 and 2.

Table 1. Chemical composition of ceramic mixtures G and R (oxides wt%).

Components	G (wt%)	R (wt%)
LOI	2.95	4.45
SiO_2	79.0	75.0
Al_2O_3	13.0	15.0
TiO_2	0.23	0.55
Fe_2O_3	0.16	0.76
CaO	1.27	0.47
MgO	0.02	0.12
K_2O	0.99	2.03
Na_2O	1.77	0.79
SO_3	0.10	0.20
ZrO_2	0.40	0.07

Table 2. Heavy metals in chemical composition of ceramic mixtures G and R (oxides mg/kg).

Components	G (mg/kg)	R (mg/kg)
CdO	12	13
Cr_2O_3	27	67
CuO	8	6
NiO	<5	<5
MnO_2	20	121
ZnO	<5	111
V_2O_5	39	74
CoO	<5	<5
BaO	103	282
PbO	<20	<20

An aqueous solution enriched with metallic silver (2.9–4.9 wt%), characterized by an alkaline pH (8.3–9.3) and low density (1.05–1.10 g/cm^3), was used as the antibacterial treatment. The solution was industrially applied on 25×25 cm^2 ceramic supports before firing, at a concentration of 90–91 g/m^2. Firing was performed at 1250 °C for 39 min total duration (cold to cold) for all tiles. After firing, specimens of 5×5 cm^2 were cut to be tested.

The tested samples were identified using acronyms referring to the fired untreated ceramic tiles (G and R) and the silver-based antibacterial treatment (A). A further code denotes the application of the treatment, which was directly deposited by serigraphic technique onto the ceramic support, as without (A1 samples) or with (A2 samples) a polymeric primer. The latter was an organic suspension with pH in the range of 6.2–7.2 and a density of 1.00–1.05 g/cm^3. The primer was sprayed onto the ceramic surface (at a concentration of about 50 g/m^2) just before the application of the antibacterial treatment. The schema of the two antibacterial systems is shown in Figure 1.

The antibacterial activity of the tiles was assessed against *Escherichia* (*E.*) *coli* strain ATCC8739, mostly following the procedure described in the standard ISO 21196:2011 [36]. Briefly, after sterilization in 70% ethanol, the tiles (with and without silver, i.e., the control sample) were inoculated with 400 µL of bacterial culture, grown up to a final concentration of ~1×10^6 CFU/mL, in nutrient broth (NB), under shaking (150 rpm), at 37 °C. A ~0.1 mm-thick sterile polypropylene film was placed upon the inoculum on the tile to prevent dehydration and optimize bacterial contact with the tile. Following incubation at 37 °C for 24 h, 10 mL of soybean casein digest broth, containing lecithin and polyoxyethylene sorbitan monooleate (SCDLP), was used to collect the bacteria from each

tile; colony-forming units (CFU) were enumerated after spreading serial dilutions of the initial suspension on Luria Bertani (LB) agar (15 g/L) medium. Each test was conducted in triplicate. The antibacterial activity (R-value) was calculated using the following equation: $R = (U_t - U_0) - (A_t - U_0) = U_t - A_t$, where U_0 and U_t are the averages of the log (i.e., base 10 logarithm) of the number of CFU/cm^2 recovered from the tiles without silver, immediately after inoculation and after 24 h, respectively; A_t is the average of the log of the number of CFU/cm^2 recovered from the tiles with silver after 24 h. Each test was considered valid when the following equation was satisfied: $(L_{max} - L_{min})/(L_{mean}) \leq 0.2$ where L_{max}, L_{min}, and L_{mean} are the log of the maximum, minimum, and mean number of CFU found on the tile without silver immediately after inoculation, respectively.
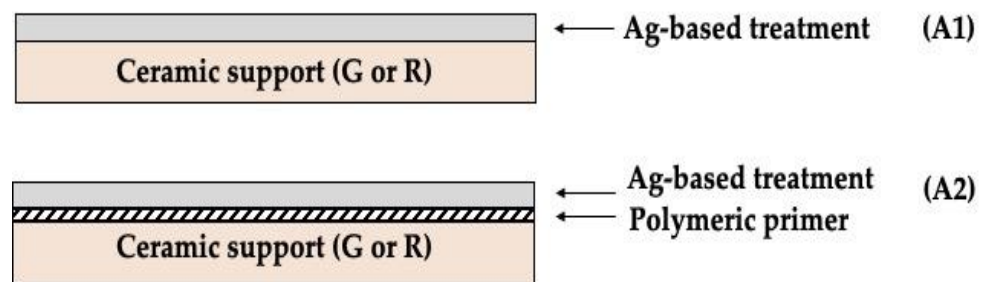
Figure 1. Schema of the investigated antibacterial systems.

Evaluation of stain resistance was carried out on all the samples by the method described in EN ISO 10545-14:2015 [37]. Staining agents (chrome green paste, alcoholic iodine solution (13 g/L), and olive oil) and cleaning procedures were applied to classify the samples' surface on the basis of detectable visual changes. Five levels of classification (from 5 to 1, respectively, the highest- and the lowest-performing) were used, as required in EN ISO 10545-14:2015.

The "sessile drop" technique was used to measure the wettability parameter of all the surface samples, using a multi-apparatus instrument, according to EN 15802:2010 [38]. Five drops, 2 μL in volume, of distilled water (wetting liquid) were uniformly deposited on the surfaces of the samples and singly captured. The average value of the contact angle was then derived, computing the uncertainty as the standard deviation for each samples' surface. By means of appropriate image-processing software, the contact angle was geometrically obtained by fitting the droplet's circular profile with a mathematical algorithm and calculating the angular coefficient of the tangent passing through the triple point (liquid-surface-air tensions).

Morphological and textural characteristics of the ceramic surfaces were evaluated using an optical profiler (LEICA DCM 3D, Heerbrugg, Switzerland), set on a metrological system (point autofocus profiling). The objective was set to $10\times$ magnification to acquire, for each sample, an area of 4.66 mm $\times$ 4.36 mm with a 452 μm vertical scanning interval. Representative 3D elaborations were obtained, and numerical data were extrapolated in terms of peak density (Spd), according to ISO 25178-2:2012 [39]. In addition, 2D profiles were extrapolated from the acquired areas to obtain useful parameters such as average surface roughness (Ra), maximum peak height (Rp), and maximum valley depth (Rv), according to ISO 4287:2009 [40]. Microstructural and compositional surface information was obtained using scanning electron microscopy (SEM). Imaging was carried out using a field emission gun (FEG) instrument (Tescan, Mira3, Brno, Czech Republic), applying a working distance of 10 mm and a voltage of 10 kV. Microanalysis was performed using a scanning electron microscope (ZEISS EVO 40, Oberkochen, Germany) coupled with an energy dispersion spectroscopy system (EDS, Inca, Oxford, UK). All the samples were gold-coated before observation to make them conductive.

3. Results and Discussion

All the ceramic tiles tested in this work showed antibacterial activity against *E. coli* ATCC8739 (Table 3). In particular, G-A1, G-A2, and R-A2 showed strong antibacterial activity against this strain (bacterial reduction of 99.999% and R-values > 5.6), while R-A1 showed a lower effect, with an antibacterial activity of 99.71% and R-value > 2.5. The R-value of 5.88 corresponded to the absence of viable cells countable after the treatment.

Table 3. Antibacterial activities of the tiles tested in this work against *E. coli* ATCC8739.

	G-A1	G-A2	R-A1	R-A2
Bacterial reduction	99.999%	99.999%	99.71%	99.999%
R-value	5.880 ± 0.084	5.880 ± 0.084	2.538 ± 0.140	5.647 ± 0.008

These results indicate that the lack of a priming polymeric layer in A1 lowers the antimicrobial activity of porcelain stoneware tiles containing a high percentage of recycled material (R). Thus, although the antimicrobial activity of the R-type tiles was significant (R > 2.5), the presence of a polymeric primer seemed to further improve the final antimicrobial activity. Conversely, the absence of a polymeric base did not affect the antimicrobial efficacy of tiles made with typical raw materials (G).

Table 4 shows the stain-resistance classification of the investigated samples according to ISO 10545-14. Samples without antibacterial treatments were also tested as reference samples, with three staining agents (e.g., chrome green paste, alcoholic iodine solution, and olive oil, which were used to feature three different types of stains: powder, oxidizing, and film, respectively). All surfaces exhibited the maximal level of resistance to the oxidizing staining action, falling within class 5 for the iodine solution. Both G-A2 and R-A2 samples, to which antibacterial treatment was applied with a primer, exhibited the highest classification for all the staining agents, with results equal to or better than A1 and untreated samples.

Table 4. Stain resistance classes defined for the test samples according to ISO 10545-14.

Sample	CHROME *	IODINE	OIL
G	4	5	4
G-A1	4	5	4
G-A2	5	5	5
R	4	5	4
R-A1	4	5	3
R-A2	5	5	4

* The test is deemed to have also been passed if an oily halo remains, providing there is no longer visible green pigmentation.

The lowest class observed for stain resistance (class 3) was only attributed to the R-A1 sample when oil removal was tested, for which a deeper cleaning action was necessary to completely remove a light halo left by the film-staining agent.

Table 5 shows the average values of the contact angle measured for each sample. Overall, considering the standard deviation, these values fell within the range of 55–73°, which corresponds to an intermediate wettability degree for all of the surfaces under analysis. In general, this wetting behavior is typical for porcelain stoneware tiles [41].

Table 5. Average contact angle values and respective standard deviation for the analyzed samples.

	G	G-A1	G-A2	R	R-A1	R-A2
Contact angle (°)	60 ± 5	63 ± 7	62 ± 6	69 ± 3	65 ± 7	69 ± 4

Figure 2 shows the 3D topography scale models of the scanned areas of the analyzed surfaces. By comparing the reported topographies, it was noticeable that all surfaces were characterized by a heterogeneous structure due to a high absolute value of the gap between peaks and pits. This texture is in line with the productive process of unglazed ceramic tiles, which have a prominent micro-roughness [41].

G

R

G-A1

R-A1

G-A2

R-A2
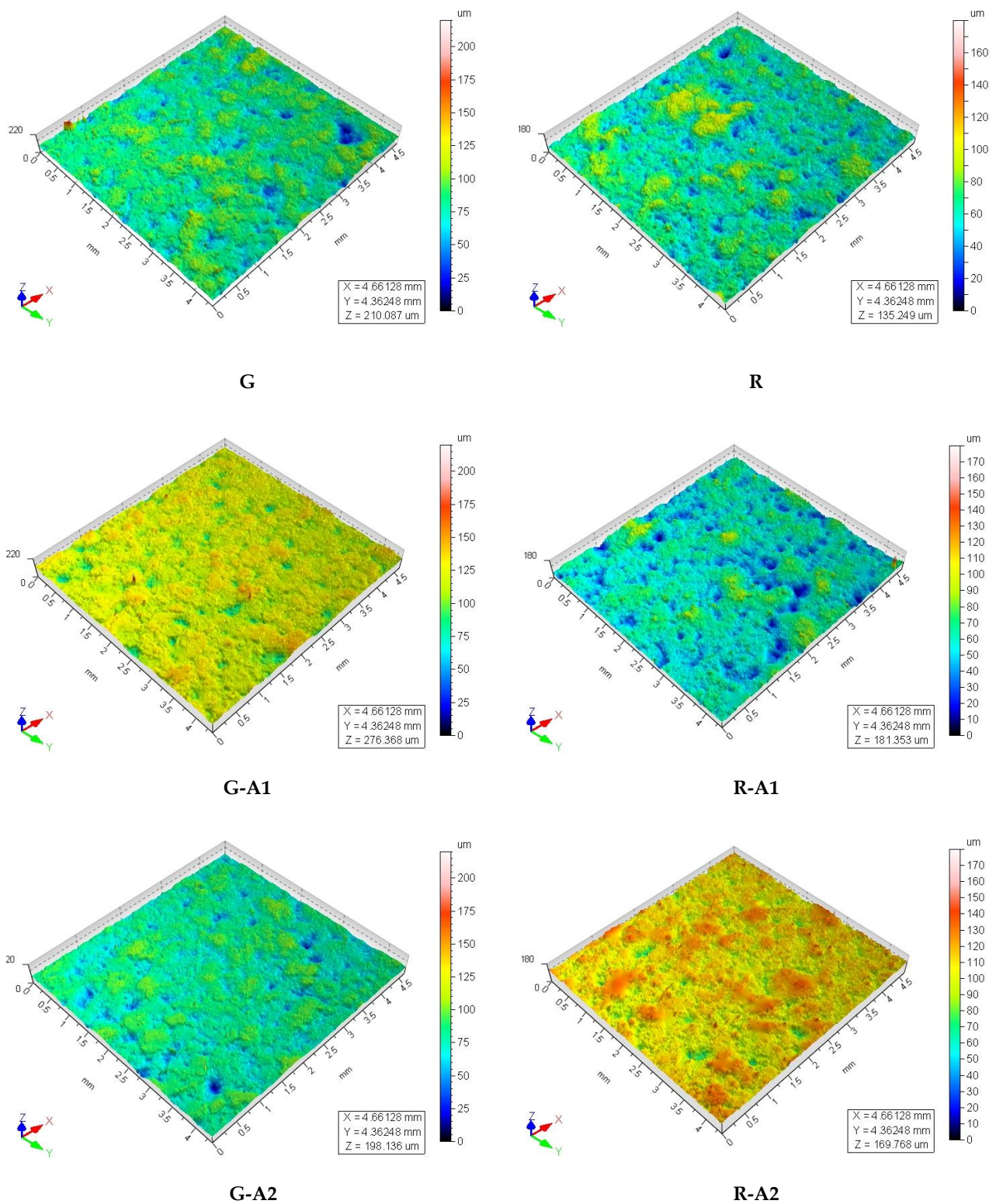
Figure 2. Graphic 3D elaborations of the investigated portion of the samples' surface.

The roughness parameters values, reported in Table 6, were not significantly different between untreated and treated samples. Moreover, in both G and R samples, the peak density, Spd, was slightly lower in treated samples than in untreated ones, with lower values in the A1-treated type, which was functionalized with only the silver treatment, i.e., without a primer layer. This aspect, which did not influence the antibacterial efficacy

of the tested treatment, indicates that the silver-based treatment alone allowed a slightly smoother and more homogenous ceramic surface. Overall, the values of this parameter were higher for the R samples as compared to the G samples.

Table 6. Roughness parameters (Ra, Rv, Rp, and Spd) obtained by profilometric analysis on all the samples.

Parameter	Description	G	G-A1	GA2	R	R-A1	R-A2
Ra (μm)	Average roughness	4.8 ± 0.7	4.3 ± 0.6	4.6 ± 0.8	4.3 ± 0.8	4.4 ± 0.8	4.3 ± 0.6
Rv (μm)	Maximum valley depht	13 ± 3	12 ± 3	14 ± 4	12 ± 3	12 ± 3	12 ± 2
Rp (μm)	Maximum peak height	11 ± 2	10 ± 3	10 ± 2	10 ± 2	10 ± 2	12 ± 2
Spd (1/mm^2)	Density of peaks	9.0	4.8	7.5	17.6	8.4	10.0

Comparing the contact angle with the roughness values, some correspondence was appreciable. Similar to the average roughness (Ra), the contact angle and surface roughness values (except for the density of peaks, Spd) were comparable, also considering the standard deviation, in untreated and treated samples. These results indicate that silver-based antibacterial treatment did not influence the surface characteristics of the porcelain stoneware tile. Moreover, the scattering present in the results of both contact angle and average roughness was attributable to the heterogeneous nature of ceramic surfaces, which could cause significant spotted variations in measurements.

Even if it was not evident from the reported numerical roughness parameters, the 3D image of the R-A1 sample (Figure 2) seemed to be characterized by larger and deeper valleys compared to the other samples' images. This feature could be responsible for the worse antibacterial efficiency and stain resistance of this sample to oil, as reported in Tables 3 and 4, respectively. Indeed, grooved surfaces provide a favorable interface for bacterial colonization and the formation of biofilm. Biofilms are clusters of bacteria that are attached to a surface and are embedded in a self-produced matrix that provides protection against antimicrobial compounds and other environmental stresses [42].

The SEM images in Figures 3–5 show representative surfaces of the investigated samples at different magnifications. They revealed crystalline structures submerged in a vitreous matrix (flatter and smoothest portions), and, overall, a heterogeneous microstructure was noted in all the observed samples, confirming the previous surface features measured by profilometry (Table 6). This microstructure is typical of unglazed porcelain stoneware surfaces [43]. Detrital materials incoherent with the matrix were often observed, which could probably be related to particle fouling from the manufacturing process. Samples based on the G mix exhibited smoother surfaces compared to the relevant samples based on the R mix, except for samples G-A2 and R-A2, which looked very similar.
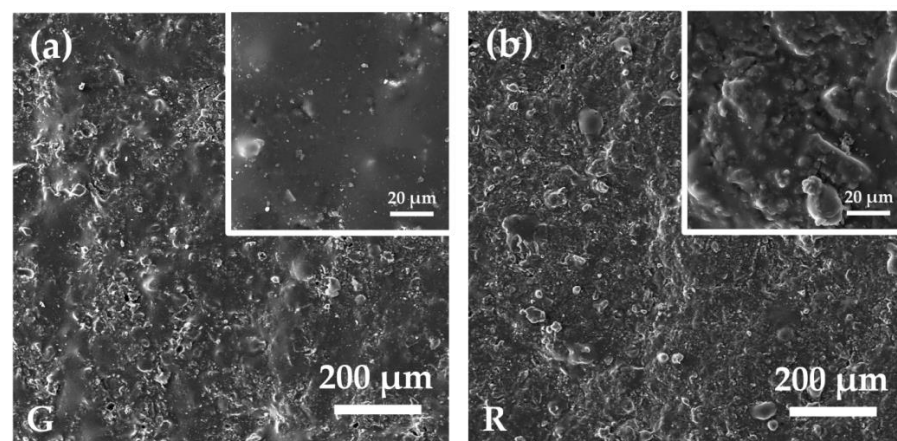
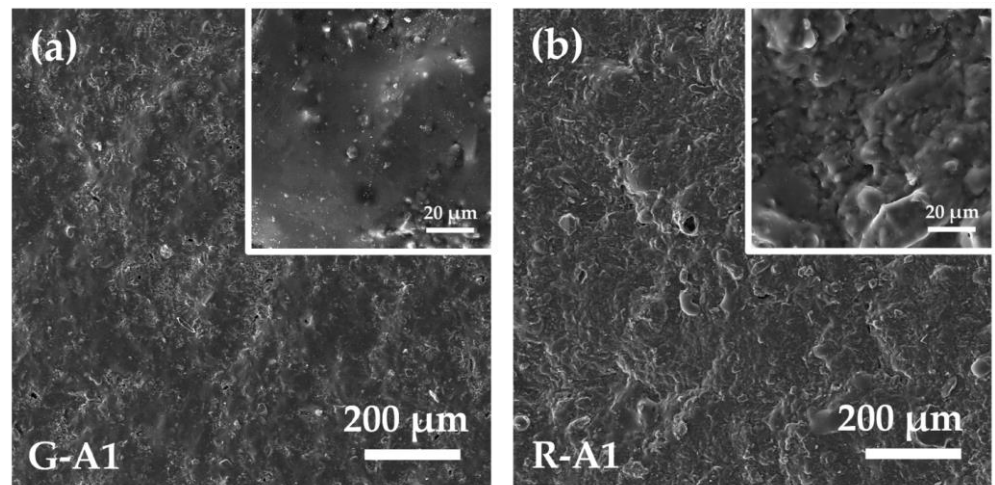**Figure 3.** SEM images of G (**a**) and R (**b**).

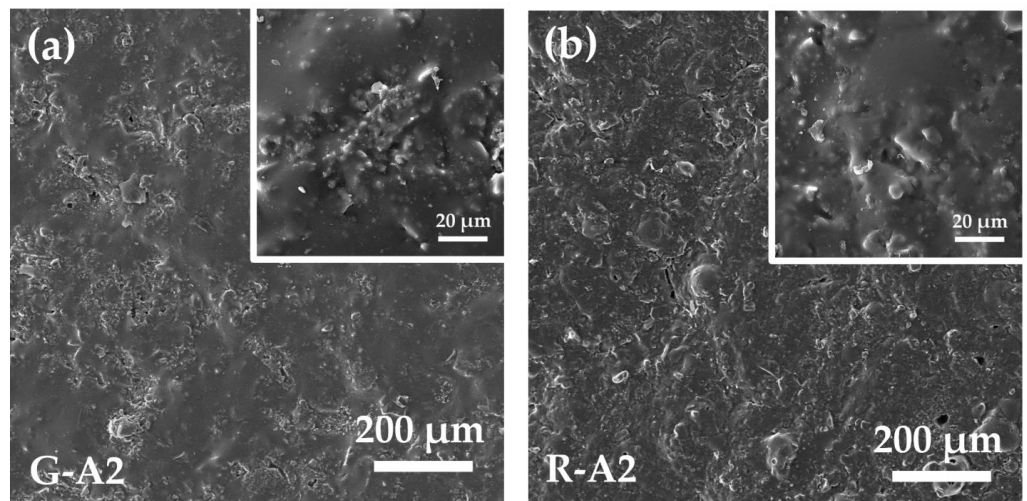**Figure 4.** SEM images of G-A1 (**a**) and R-A1 (**b**).

Figure 5. SEM images of G-A2 (**a**) and R-A2 (**b**).

Lastly, by observing the EDS spectra of all the surfaces in Figure 6, it was evident that the main compositional difference was the presence of Zircon (Zr) in G samples respective to R samples. This was related to the different compositions of raw materials used in G and R mixes. Indeed, the concentration of the detected elements (and therefore peak height) confirmed the weight percentages reported in Table 1. Conversely, silver was not experimentally or analytically detectable due to the low concentration applied (about 90 g/m^2) and the limited sensitivity of EDS analysis. In particular, by broadening the spectra, the acquisition software suggests that, if traceable, silver would give peaks for values of 2.98 and 3.15 keV, as shown in Figure 7.
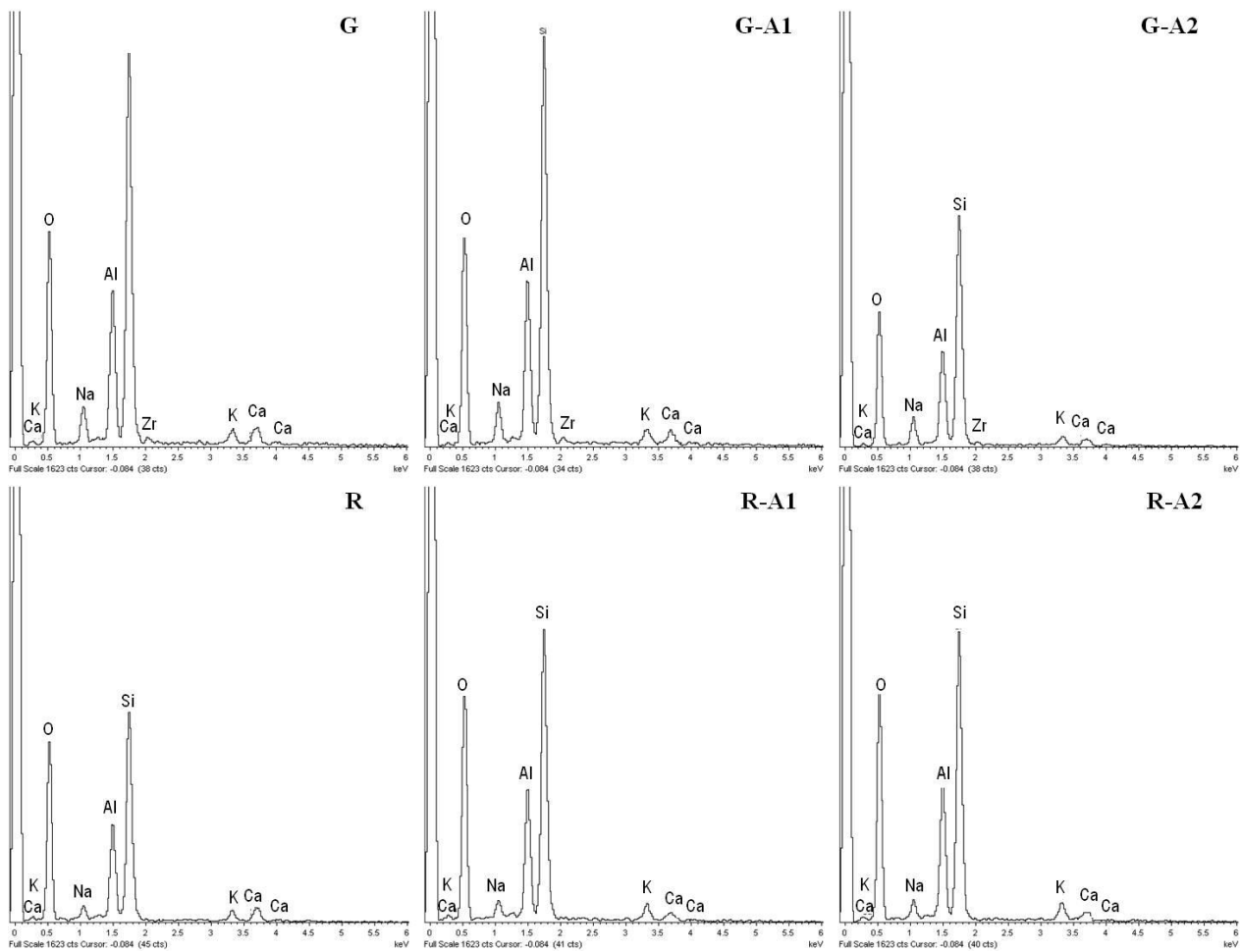
Figure 6. EDS spectra of treated samples G, G-A1, G-A2 and R, R-A1, R-A2.
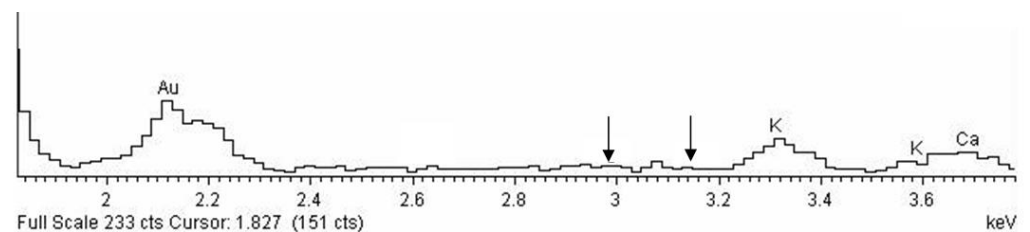

Figure 7. Enlarged EDS spectrum of the treated sample G-A1. The arrows indicate the keV typical of silver.

4. Conclusions

The results of this research allowed the evaluation of sustainable ceramic tiles with a high content of recycled material (R) in terms of high antibacterial efficacy, compared to traditional tiles without any waste material (G).

The silver-based functionalizing treatment (A1), applied with a screen-printing technique, proved to be effective for both types of ceramic substrate, even if a bit less for the R-A1 (99.71%) sample compared to G-A1 (99.999%). The addition of a polymeric primer (A2) improves performance in terms of microstructure and texture of the ceramic surface after firing. In particular, the microstructural and textural analyses showed that the cleanability (stain resistance) and antibacterial properties of porcelain stoneware tiles depend on surface characteristics such as roughness parameters.

In the specific case of the R-A1 sample, for which the antibacterial efficacy and stain resistance are the lowest, profilometry analysis, returned by 3D processing, highlights a greater number of valleys characterized by a slightly larger width than the surfaces of the other samples, and textural parameters showed the lowest Spd value (density of peaks) among the samples of the R series. Indeed, grooved surfaces offer an optimal substrate for bacterial adhesion and protection due to biofilm formation.

In conclusion, the correlation among data obtained from different experimental techniques highlights the importance of a multi-analytical approach for the definition of the surface performance of ceramic tiles. Moreover, our results showed that, independently of the body mix composition (with or without recycled raw materials), porcelain stoneware tiles can achieve strong antibacterial properties, indicating the possibility of the production of sustainable ceramics with a broad application range.

Author Contributions: Conceptualization, E.R.; methodology, V.L.T., E.R., G.M., S.N., D.G. and M.C..; formal analysis, D.G.; investigation, V.L.T. and S.N.; data curation, V.L.T.; writing—original draft preparation, V.L.T., G.M., E.R., S.N., D.G. and M.C.; writing—review and editing, E.R., G.M., M.C., D.G. and M.C.B.; supervision, for the experimental work E.R. and M.C.B., for the microbiological analysis M.C. All authors have read and agreed to the published version of the manuscript.

Institutional Review Board Statement: Not applicable.

Informed Consent Statement: Not applicable.

Data Availability Statement: Not applicable.

Conflicts of Interest: The authors declare no conflict of interest.

References

1. Sciancalepore, C.; Manfredini, T.; Bondioli, F. Antibacterial and self-cleaning coatings for silicate ceramics: A review. *Adv. Nat. Sci. Nanosci. Nanotechnol.* **2019**, *92*, 90–99.
2. Seabra, M.P.; Grave, L.; Oliveira, C.; Alves, A.; Correia, A.; Labrincha, J.A. Porcelain stoneware tiles with antimicrobial action. *Ceram. Int.* **2014**, *40*, 6063–6070. [CrossRef]
3. Berto, A.M. Ceramic tiles: Above and beyond traditional applications. *J. Eur. Ceram. Soc.* **2007**, *27*, 1607–1613. [CrossRef]
4. Welch, K.; Sloan, G.; Ong, I.; Microban International. Antimicrobial Treatment for Ceramics and Sanitary Ware. *World Ceram. Rev.* **2017**, *121*, 104–108.
5. Bianchi, C.L.; Cerrato, G.; Bresolin, B.M.; Djellabi, R.; Rtimi, S. Digitally printed AgNPs doped TiO$_2$ on commercial porcelain-grès tiles: Synergistic effects and continuous photocatalytic antibacterial activity. *Surfaces* **2020**, *3*, 11–25. [CrossRef]
6. Baheiraeia, N.; Moztarzadeha, F.; Hedayati, M. Antibacterial Ag/SiO$_2$ thin film on glazed ceramic tiles prepared by sol-gel method. In Proceedings of the 18th Iranian Conference of Biomedical Engineering (ICBME), Tehran, Iran, 14–16 December 2011; IEEE: Piscataway, NJ, USA, 2011; pp. 105–108.
7. Bondioli, F.; Manfredini, T. Le nanopolveri nella funzionalizzazione delle superfici ceramiche. *Ceram. Inf.* **2008**, *468*, 231–237.
8. Slavin, Y.N.; Asnis, J.; Häfeli, U.O.; Bach, H. Metal nanoparticles: Understanding the mechanisms behind antibacterial activity. *J. Nanobiotechnology* **2017**, *15*, 65. [CrossRef]
9. Raghunath, A.; Perumal, E. Metal oxide nanoparticles as antimicrobial agents: A promise for the future. *Int. J. Antimicrob. Agents* **2017**, *49*, 137–152. [CrossRef]
10. Martinez-Gutierrez, F.; Olive, P.L.; Banuelos, A.; Orrantia, E.; Nino, N.; Sanchez, E.M.; Ruiz, F.; Bach, H.; Av-Gay, Y. Synthesis, characterization, and evaluation of antimicrobial and cytotoxic effect of silver and titanium nanoparticles. *Nanomedicine* **2010**, *6*, 681–688. [CrossRef]
11. Simon-Deckers, A.; Loo, S.; Mayne-L'hermite, M.; Herlin-Boime, N.; Menguy, N.; Reynaud, C.; Gouget, B.; Carriere, M. Size-, composition- and shape-dependent toxicological impact of metal oxide nanoparticles and carbon nanotubes toward bacteria. *Environ. Sci. Technol.* **2009**, *43*, 8423–8429. [CrossRef]
12. Karakoti, A.S.; Hench, L.L.; Seal, S. The potential toxicity of nanomaterials—The role of surfaces. *JOM* **2006**, *58*, 77–82. [CrossRef]
13. Choi, O.; Hu, Z. Size dependent and reactive oxygen species related nanosilver toxicity to nitrifying bacteria. *Environ. Sci. Technol.* **2008**, *42*, 4583–4588. [CrossRef] [PubMed]
14. Sohm, B.; Immel, F.; Bauda, P.; Pagnout, C. Insight into the primary mode of action of TiO$_2$ nanoparticles on Escherichia coli in the dark. *Proteomics* **2015**, *15*, 98–113. [CrossRef] [PubMed]
15. Fujishima, A.; Zhang, X.; Tryck, D.A. TiO$_2$ photocatalysis and related surface phenomena. *Surf. Sci. Rep.* **2008**, *63*, 515–582. [CrossRef]

16. Franzoni, E.; Bignozzi, M.C.; Rambaldi, E. TiO$_2$ in the building sector. In *Titanium Dioxide (TiO$_2$) and Its Applications*; Parrino, F., Palmisano, L., Dean, M., Eds.; Elsevier: Amsterdam, The Netherlands, 2021; pp. 449–479.

17. Chouirfa, H.; Bouloussa, H.; Migonney, V.; Falentin-Daudré, C. Review of titanium surface modification techniques and coatings for antibacterial applications. *Acta Biomater.* **2019**, *83*, 37–54. [CrossRef]

18. Barmeh, A.; Nilforoushan, M.R.; Otroj, S. Wetting and photocatalytic properties of Ni-doped TiO$_2$ coating on glazed ceramic tiles under visible light. *Thin Solid Film.* **2018**, *666*, 137–142. [CrossRef]

19. Da Silva, A.L.; Dondi, M.; Raimondo, M.; Hotza, D. Photocatalytic ceramic tiles: Challenges and technological solutions. *J. Eur. Ceram. Soc.* **2018**, *38*, 1002–1017. [CrossRef]

20. Durán, N.; Durán, M.; de Jesus, M.B.; Seabra, A.B.; Fávaro, W.J.; Nakazato, G. Silver nanoparticles: A new view on mechanistic aspects on antimicrobial activity. *Nanomedicine* **2016**, *12*, 789–799. [CrossRef]

21. Epple, M.; Chernousova, S. Silver as Antibacterial Agent: Ion, Nanoparticle, and Metal. *Angew. Chem. Int.* **2013**, *52*, 1636–1653.

22. Jung, W.K.; Koo, H.C.; Kim, K.W.; Shin, S.; Kim, S.H.; Park, Y.H. Antibacterial Activity and Mechanism of Action of the Silver Ion in *Staphylococcus aureus* and *Escherichia coli*. *Appl. Environ. Microbiol.* **2008**, *74*, 2171–2178. [CrossRef]

23. Sim, W.; Barnard, R.T.; Blaskovich, M.A.T.; Ziora, Z.M. Antimicrobial Silver in Medicinal and Consumer Applications: A Patent Review of the Past Decade (2007–2017). *Antibiotics* **2018**, *7*, 93. [CrossRef]

24. Sheng, H.; Congqin, N.; Yue, Z.; Lei, C.; Kaili, L.; Jiang, C. Antibacterial Activity of Silicate Bioceramics. *J. Wuhan Univ. Technol.-Mat. Sci. Edit.* **2011**, *26*, 226–230.

25. Kummala, R.; Brobbey, K.J.; Haapanen, J.; Mäkelä, J.M.; Gunell, M.; Eerola, E.; Huovinen, P.; Toivakka, M.; Saarinen, J.J. Antibacterial activity of silver and titania nanoparticles on glass surfaces. *Adv. Nat. Sci. Nanosci. Nanotechnol.* **2019**, *10*, 015012. [CrossRef]

26. Petronella, F.; Truppi, A.; Striccioli, M.; Curri, M.L.; Comparelli, R. Photocatalytic Application of Ag/TiO$_2$ Hybrid Nanoparticles. In *Noble Metal-Metal Oxide Hybrid Nanoparticles, Fundamentals and Applications*; Satyabrata Mohapatra, Phuong Nguyen-Tri, Tuan Anh Nguyen; Elsevier: Amsterdam, The Netherlands, 2019; pp. 373–394.

27. Durango-Giraldo, G.; Cardona, A.; Zapata, J.F.; Santa, J.F.; Buitrago-Sierra, R. Titanium dioxide modified with silver by two methods for bactericidal applications. *Helyon* **2019**, *5*, e01608. [CrossRef]

28. Djellabi, R.; Basilico, N.; Delbue, S.; D'Alessandro, S.; Parapini, S.; Cerrato, G.; Laurenti, E.; Falletta, E.; Bianchi, C.L. Oxidative inactivation of SARS-CoV-2 on Photoactive AgNPs@TiO$_2$ Ceramic Tiles. *Int. J. Mol. Sci.* **2021**, *22*, 8836. [CrossRef]

29. Confindustria Ceramica. *Indagini Statistiche Sull'industria Italiana*; Confindustria Ceramica: Sassuolo, Italy, 2020; pp. 8–35.

30. Palmonari, C. *Il Grès Porcellanato*; Centro Ceramico: Bologna, Italy, 1989.

31. Zannini, P. Treatments for ceramic surfaces. *Ceram. World Rev.* **2014**, *107*, 62–64.

32. Dondi, M.; Garcia-Ten, J.; Rambaldi, E.; Zanelli, C.; Vicent-Cabedo, M. Resource efficiency versus market trends in the ceramic tile industry: Effect on the supply chain in Italy and Spain. *Resour. Conserv. Recycl.* **2021**, *168*, 105271. [CrossRef]

33. Rambaldi, E.; Esposito, L.; Tucci, A.; Timellini, G. Recycling of polishing porcelain stoneware residues in ceramic tiles. *J. Eur. Ceram. Soc.* **2007**, *27*, 3509–3515. [CrossRef]

34. Rambaldi, E.; Fazio, S.; Prete, F.; Bignozzi, M.C. Innovative ceramic tile mixes. *Cfi/Ber. DKG* **2016**, *93*, 57–60.

35. Rambaldi, E. Pathway towards a high recycling content in traditional ceramics. *Ceramics* **2021**, *4*, 486–501. [CrossRef]

36. International Organization for Standardization, ISO 22196: Measurement of antibacterial activity on plastics and other non-porous surfaces. International Organization for Standardization: Geneva, Switzerland. 2011. Available online: https://www.iso.org/standard/54431.html (accessed on 20 July 2020).

37. International Organization for Standardization, ISO10545-14: Ceramic tiles-Part14: Determination of resistance to stains.International Organization for Standardization: Geneva, Switzerland. 2015. Available online: https://www.iso.org/standard/60972.html (accessed on 20 June 2021).

38. Comité Euroéen de Notmalisation, EN 15802: Conservation of cultural property-test methods-Determinaation of static contact angle. Comité Euroéen de Notmalisation: Bruxelles, Belgium. 2010. Available online: https://standards.iteh.ai/catalog/standards/sist/c3a0a8e7-5437-499a-89e2-c4355aae5534/sist-en-15802-2010 (accessed on 20 June 2021).

39. International Organizatio for Standardization, ISO 25178-2: Geometrical Product Specifications (GPS)—Surface Texture: Areal—Part 2: Terms, Definitions and Surface Texture Parameters. International Organization for Standardization: Geneva, Switzerland. 2012. Available online: https://www.iso.org/standard/42785.html (accessed on 20 March 2021).

40. Intenational Organization for Standardization, ISO 4287: Geometrical Product Specifications (GPS)—Surface Texture: Profile Method—Terms, Definitions and Surface Texture Parameters; International Organization for Standardization: Geneva, Switzerland. 2009. Available online: https://www.iso.org/standard/10132.html (accessed on 20 March 2021).

41. Rambaldi, E.; Lucchese, B.; Engels, M.; Bignozzi, M.C. Evaluation of durability and cleanability performances of protective treatments for lapped ceramic tiles—Part 2. *Int. J. Appl. Ceram. Tech.* **2018**, *16*, 625–637. [CrossRef]

42. Donlan, R.M.; Costerton, J.W. Biofilm: Survival mechanisms of clinically relevant microorganisms. *Clin. Microbiol. Rev.* **2002**, *15*, 167–193. [CrossRef] [PubMed]

43. Dondi, M.; Ercolani, G.; Guarini, G.; Melandri, C.; Raimondo, M.; Rocha e Almedra, E.; Tenorio Cavalcante, P.M. The role of surface microstructure on the resistance to stains of porcelain stoneware tiles. *J. Eur. Ceram. Soc.* **2005**, *24*, 357–365. [CrossRef]